# CAELI WATER VAPOUR RAMAN LIDAR CALIBRATION AT THE CABAUW EXPERIMENTAL SITE FOR ATMOSPHERIC RESEARCH

**Arnoud Apituley, Fred Bosveld, Henk Klein Baltink, Keith M. Wilson**

*KNMI, P.O. Box 201, 3730 AE De Bilt, The Netherlands, E-mail: apituley@knmi.nl*

## ABSTRACT

Water vapour is a crucial parameter in atmospheric physics. Concentrations are low at upper tropospheric altitudes, but radiation effects are sensitive to water vapour abundance at these levels. Obtaining reliable data of low water vapour concentrations in the upper troposphere is challenging. The Raman lidar technique for water vapour can meet this challenge, however, the Raman lidar water vapour data rely on an external source for calibration. For the Raman lidar Caeli in Cabauw, operational radiosondes launched in De Bilt, about 22 km North-East of the lidar location are routinely used for this. Differences in space and time between the observations influence the consistency and quality of the calibration.

Various in-situ and remote observations of humidity are available at Cabauw that are better collocated and synchronised with the lidar measurements. These collocated observations could also be used for the lidar calibration as an alternative to the radio soundings. Among the possibilities are GNSS and microwave radiometer and tower based in-situ humidity measurements. In this paper we explore the possibilities for applying those for the Raman lidar calibration in Cabauw.

## 1. INTRODUCTION

As atmospheric temperatures increase due to the continued anthropogenic injection of carbon dioxide, it is expected that water vapour concentrations will increase as well, inducing an enhancement of the greenhouse effect. All climate models predict this enhancement, but diversity in sensitivity to changes in radiative perturbations is present amongst the models [6]. Upper tropospheric water vapour, i.e. water vapour between the levels of 250 – 400 hPa plays a special role in our climate. Even though the amount of water vapour at those levels is small, the sensitivity of the outgoing radiation to water vapour is dominated by upper-tropospheric water vapour [13]. Consequently, it is of great importance to accurately record the upper tropospheric water vapour.

The low concentrations of water vapour in the upper troposphere and lower stratosphere (UTLS) make measurement at these altitudes very difficult. The sensitivity of operational radiosonde sensors suffers under conditions of very low ambient temperatures and relative humidities, limiting the range of high quality measurements to the low and middle troposphere [8]. Research-grade balloonborne frost-point hygrometers remain the best source of high quality water vapour measurements in the UTLS [15] but are too expensive to be used on an operational basis. Also, satellite measurement uncertainties remain high near the tropopause due to the abrupt change of mixing ratio at the tropopause level [10]. Due to the capabilities of Raman lidar for monitoring water vapour at low concentrations [7] it is being adopted in networks such as NDACC [9] and the GCOS Reference Upper Air Network (GRUAN) [5].

The Raman lidar observations of water vapour solely rely on the measurement of Raman lidar returns of both water vapour and of nitrogen ($N_2$). The ratio of the two lidar signals can be shown to be proportional to the water vapour to dry air mixing ratio and, in principle, only need a single point within the profile for calibration. Radiosondes are often used for this by extracting a matching range interval from the lidar and the sonde to obtain the required calibration constant. However, the launch site of the sonde may not be the same as the lidar location, and the sonde drift during ascent [12] raises the issue of representativity with respect to the lidar, especially in cases of high atmospheric variability .

At the Cabauw Experimental Site for Atmospheric Research (CESAR) in the Netherlands (51°58'N, 4°56'E), a suite of in situ and ground based remote sensing instruments are routinely operated to provide synergy in atmospheric observations. In particular, in-situ and remote observations of aerosols, clouds, radiation and precipitation related measurements are made [11]. These observations are made for both monitoring of climate change, as well as process studies. CESAR is one of the initial GRUAN sites.

Various in-situ and remote observations of humidity are available at Cabauw that are well collocated and synchronised with the lidar measurements. These observations could also be used for the lidar calibration as an alternative to the radio soundings, avoiding issues with representativity. Among the possibilities are GNSS and microwave radiometer (providing integrated column values of water vapour) and tower based in-situ humidity measurements. In this paper we explore the possibilities for applying those for the Raman lidar calibration in Cabauw.

## 2. INSTRUMENTATION

### 2.1. Caeli

Caeli is the CESAR water vapour, aerosol and cloud lidar and is set up as a multiwavelength Raman lidar [1]. It is deployed in Cabauw, as a key instrument for CESAR to strengthen the sites capabilities as a profiling station for atmospheric research and climate studies. The instrument

Figure 1: The Raman lidar Caeli in operation at the Cabauw Experimental Site for Atmospheric Research (CESAR), close to the 213 m high meteorological tower.

is part of the European AerosolResearch Lidar Network (EARLINET) [3] and is getting involved in GRUAN.

The system uses a high power frequency doubled and tripled Nd:YAG laser and emits 1064, 532 and 355 nm simultaneously. Wavelengths are detected at the elastically scattered lines, as well as the $N_2$ vibrational Raman lines at 607 and 387 nm and the water vapour vibrational Raman line at 407 nm. Measured parameters are backscatter profiles at 1064, 532 and 355 nm, extinction profiles at 607 and 387 nm, linear depolarisation ratio at 532 nm and the water vapour to dry air mixing ratio (specific humidity) $Q$.

The lidars optical receiver is at present configured with a large aperture far range telescope and a near range telescope. Both telescopes are fibre coupled to a wavelength separation box with dichroic mirrors for pre-selection of wavelengths and narrow-band interference filters for final background light suppression. Both telescopes are used to detect the full set of elastic and Raman scattered lidar signals. A separate third telescope is used for linear depolarization measurements.

The ratio of the WV Raman signal and the $N_2$ Raman signal is directly proportional to $Q$. Corrections may be necessary in case of strong aerosol loading [7] , but this correction is not routinely performed. At present, a humidity profile is obtained from both the far-range and near-range telescopes by calibration against a near-simultaneously launched radio sonde. After a range dependent smoothing, the near and far range profiles are merged into one final profile.

### 2.2. Radiosonde

Routine launches of Vaisala RS92 radiosondes are performed at the KNMI main location in De Bilt (52°6'N, 5°1'E, WMO code 0620), about 20 km East of the lidar location. Sondes are launched daily at 00 and 12 UTC.

Calculation of $Q$ from the radio sonde relative humidity, temperature and pressure data is done using formulations described by Sonntag [14].

### 2.3. Tower based humidity observations

In-situ air and dewpoint temperatures, $T_{\rm air}$ and $T_{\rm d}$, are measured at seven levels in the tower at 200, 140, 80, 40, 20, 10 and 1.5 m [2]. $T_{\rm air}$ is measured with a KNMI PT500-element in an unventilated KNMI temperature hut. At conditions with low wind speed and high irradiation this may result in overestimations of a few tenths of a degree K. $T_{\rm d}$ is measured with a Vaisala HMP243 heated relative humidity sensor with a metal filter in a separate Vaisala unventilated hut. This hut is open in construction. From April 2010 onwards, E+E sensors are used in an unventilated KNMI hut separated from the temperature measurements.The humidity data can be overestimated during drying episodes after dew, fog or rain, because of a wet shielding or sensor. This may result in observed dewpoint temperatures higher than the air temperature.

The specific humidity $Q_{\rm tower}$ is calculated from the $T_{\rm air}$ and $T_{\rm d}$ data, following [17]. For now, only the data collected at the 200 m level are considered.

## 3. RADIOSONDE VS. TALL TOWER CALIBRATION

To investigate the feasibility of using the tall tower measurements of humidity for calibrating the lidar, a simple experiment was done. A number of observations were selected with near simultaneous lidar and radio soundings during nighttime, under clear atmospheric conditions. The lidar data were calibrated against the De Bilt radio sondes using an interval between about 2 and 6 km altitude. In this region, normally both instruments perform well. The integration time of the lidar data for each profile is between one and two hours, mainly to obtain sufficient signal to noise (SNR) in the upper troposphere.

Next, the mean humidity from the sonde calibrated lidar profile in an interval between 150 and 250 m ($Q_{\rm lidar}$) were plotted on the tall tower humidity data from the 200 m level ($Q_{\rm tower}$). In case the lidar-sonde calibration provides satisfactory results for the whole profile, it can be expected that $Q_{\rm lidar}$ coincides with $Q_{\rm tower}$ at 200 m.

Examples of the results are shown in Fig.2 for a number of cases on 27 Jan. 2010 and 18–19 May 2010. The examples show at a glance that at least good correlation is obtained between lidar and tall tower observations.

## 4. DISCUSSION

The fact that $Q_{\rm lidar}$ and $Q_{\rm tower}$ compare favourably at the 200 m level is not as trivial as it may seem, since it is well known that most lidars have an incomplete overlap at close range. This is a major problem for any lidar retrieval that relies on the signal shape as a function of range, such as the aerosol extinction [16]. From EARLINET quality assurance procedures [4] it is known that the Caeli near-range telescope has a full overlap range for

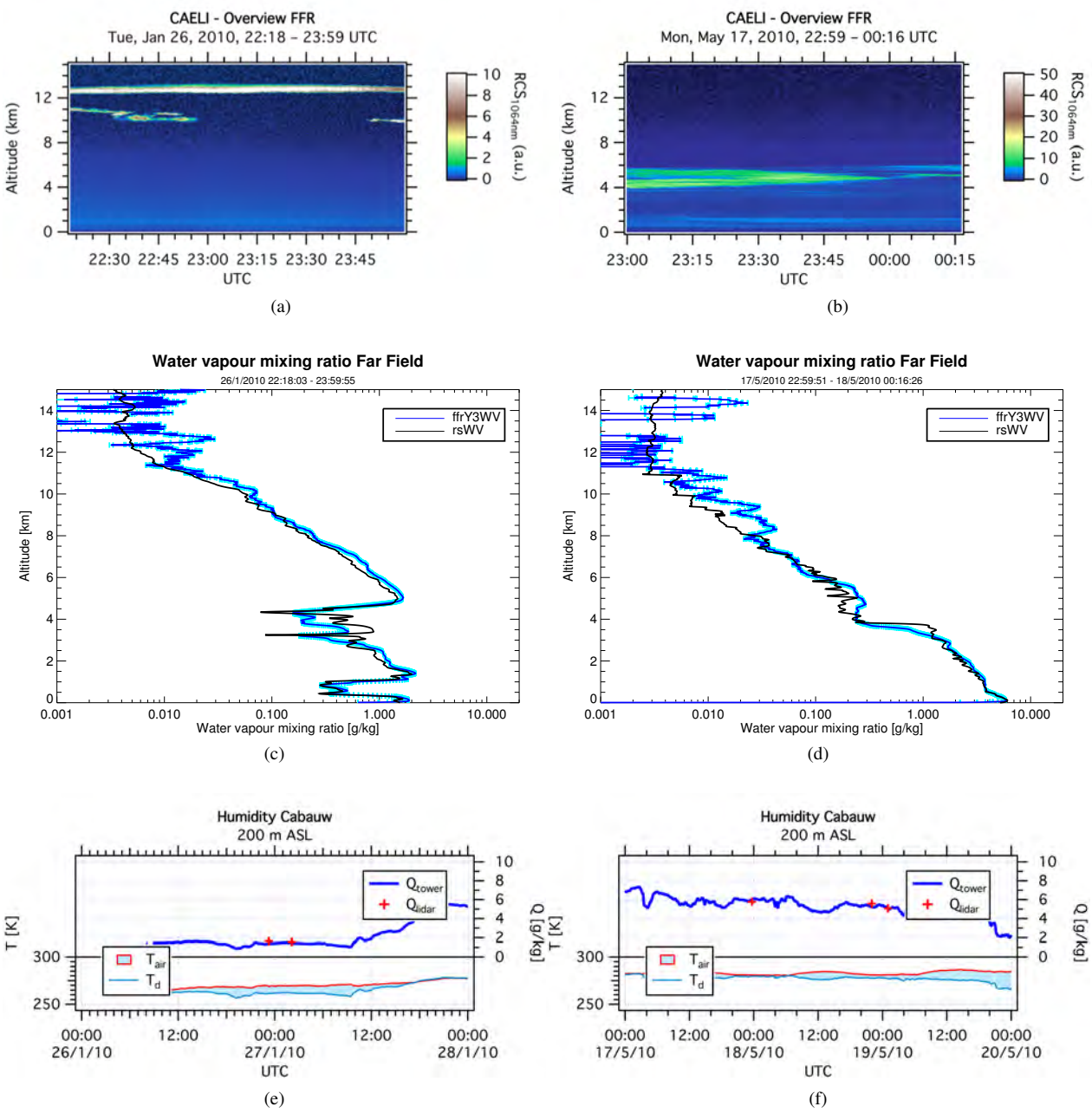


Figure 2: Overview of sample results. The atmospheric conditions are shown in the time-height plots of the range corrected lidar data (RCS) for the periods during the night of 26-27 Jan. 2010 with thin cirrus (2a) and during the night of 17-18 May 2010 with a volcanic dust layer between 4 and 6 km (2b). Lidar and sonde humidity profiles after lidar to sonde calibration are shown in the panels (2c) and (2d). In (2e) and (2f) the comparison of in-situ and lidar humidity data is shown. In the bottom part of the figure the in-situ values at the 200 m level of $T_{\mathrm{air}}$ and $T_{\mathrm{d}}$ are plotted from which $Q_{\mathrm{tower}}$ is derived. The top part of the figure shows $Q_{\mathrm{tower}}$ with a continuous line and $Q_{\mathrm{lidar}}$ indicated by markers.

355, 387 and 407 nm starting at about 500 m. However, due to the optical design of the instrument, near-identical optical paths exist in the receiver for the signals related to the same emitted wavelength; in this case 355 nm. This was experimentally verified using the EARLINET QA procedures. Since $Q_{\mathrm{lidar}}$ is obtained from a ratio of the 407 and 387 nm signals, overlap functions of both signals are expected to cancel, to some extent, due to the near-identical optical paths of the signals in the receiver. Our results show that virtually no overlap effects seem to remain at this level. Moreover, the examples also show that the results can be obtained consistently over time. More cases were analysed than shown here, giving similar results. A full analysis of the data is ongoing.

## 5. CONCLUSIONS

Raman lidar specific humidity data obtained with sonde calibration compare favourably with in-situ humidity measurements from the tall tower in Cabauw. Geometrical effects in the lidar receiver almost completely cancel out consistently due to the design and implementation of Caeli. Although a full analysis of all available data is not yet complete, is seems that long term consistency checks of the lidar humidity calibration using the in situ tower data that are well collocated and synchronised with the lidar are useful.

This paper presents work in progress. At the time of the conference, more results are expected and better founded conclusions can be drawn.

## REFERENCES


1. A. Apituley, et al. Performance assessment and application of caeli – a high-performance raman lidar for diurnal profiling of water vapour, aerosols and clouds. In A. Apituley, H. Russchenberg, and W. Monna, editors, *Proceedings of the 8th ISTP*, pages S06–O10, 2009.
2. CESAR. http://www.cesar-observatory.nl/.
3. EARLINET. http://www.earlinet.org.
4. V. Freudenthaler. The telecover test: A quality assurance tool for the optical part of a lidar system. In M. Hardesty, et al., editors, *Proceedings of the 24th ILRC*, pages 145–146. ILRC24, 2008.
5. GRUAN. http://www.gruan.org/.
6. I. M. Held and B. J. Soden. Water vapor feedback and global warming1. *Annual Review of Energy and the Environment*, 25(1):441–475, 2000.
7. T. Leblanc, et al. Measurements of humidity in the atmosphere and validation experiments (mohave)-2009: overview of campaign operations and results. *Atm. Meas. Tech.*, 4(12):2579–2605, 2011.
8. L. M. Miloshevich, et al. Accuracy assessment and correction of vaisala rs92 radiosonde water vapor measurements. *J. Geophys. Res.*, 114(D11), 06 2009.
9. NDACC. http://www.ndsc.ncep.noaa.gov/.
10. W. G. Read, et al. Aura microwave limb sounder upper tropospheric and lower stratospheric h2o and relative humidity with respect to ice validation. *J. Geophys. Res.*, 112(D24), 12 2007.
11. H. Russchenberg, et al. Ground-based atmospheric remote sensing in the netherlands: European outlook. *IEICE Transactions on Communications*, E88-B(6):2252–2258, 2005.
12. D. J. Seidel, et al. Global radiosonde balloon drift statistics. *J. Geophys. Res.*, 116(D7), 04 2011.
13. B. J. Soden and F. P. Bretherton. Upper tropospheric relative humidity from the goes 6.7 $\mu$m channel: Method and climatology for july 1987. *J. Geophys. Res.*, 98(D9):16669–16688, 1993.
14. D. Sonntag. Advancements in the field of hygrometry. *Meteorol. Zeistschrift*, 3:51–66, April 1994.
15. H. Vömel, et al. Validation of aura microwave limb sounder water vapor by balloon-borne cryogenic frost point hygrometer measurements. *J. Geophys. Res.*, 112(D24), 12 2007.
16. U. Wandinger and A. Ansmann. Experimental determination of the lidar overlap profile with raman lidar. *Appl. Opt.*, 41(3):511–514, Jan 2002.
17. D. Wetterdienst. *Aspirations-Psychrometer-Tafeln*. Vieweg, 6th edition, 1979.